Int. J. Heat Mass Transfer. Vol. 23, pp. 27–36
© Pergamon Press Ltd. 1980. Printed in Great Britain

0017-9310/80/0101-0027 $02.00/0

POOL BOILING HEAT TRANSFER FROM HORIZONTAL PLANE HEATER TO MERCURY UNDER MAGNETIC FIELD

OSAMU TAKAHASHI, MASAAKI NISHIDA, NOBUYUKI TAKENAKA and ITARU MICHIYOSHI
Department of Nuclear Engineering, Kyoto University, Kyoto, Japan

(*Received* 20 *December* 1978)

Abstract—Reproducible experimental data are presented on the pool boiling heat transfer from a horizontal plane heater to mercury under various system pressures and liquid levels in the presence of a magnetic field of which direction is parallel to the direction of gravity. With increasing the magnetic flux density, both the incipient boiling heat flux and the burnout heat flux decrease in comparison with those for the non-magnetic field. However, when the liquid thickness above the heating surface is thin, the magnetic field affects little the incipient boiling heat flux and the burnout heat flux. Results of a visual study of mercury boiling are also discussed.

NOMENCLATURE

B,	magnetic flux density [T];
H,	height of large bubble above liquid surface (see Fig. 16) [mm];
H_{max},	maximum height of large bubble above liquid surface [mm];
$L.L$,	liquid level above heating surface [mm];
q,	surface heat flux [W m^{-2}];
q_{IB},	incipient boiling heat flux [W m^{-2}];
$q_{IB\,B=0}$,	incipient boiling heat flux under non-magnetic field [W m^{-2}];
q_{crit},	burnout heat flux [W m^{-2}];
$q_{crit\,B=0}$,	burnout heat flux under non-magnetic field [W m^{-2}];
S.P.,	system pressure [torr];
T_l,	liquid temperature [°C];
T_{sat},	saturation temperature corresponding to system pressure [°C];
T_w,	heating surface temperature [°C];
$T_{w\,sat}$,	saturation temperature corresponding to system pressure plus liquid level above heating surface [°C];
α,	heat-transfer coefficient [W m^{-2}K^{-1}].

INTRODUCTION

IN GENERAL, the characteristic of pool boiling heat transfer is much dependent on the motion of liquid and bubbles adjacent to the heating surface. Such a motion of liquid is affected by the Lorentz force, if the electrically conducting liquid, for example liquid metal, moves under an applied magnetic field. Therefore, it is expected that the magnetic field affects the natural convection heat transfer, the inception of boiling, the velocity field generated by growing and moving bubbles, and thus the characteristic of heat transfer. Boiling in thin liquid layer is also an interesting problem.

The literature survey with respect to the natural convection and pool boiling heat transfer in the presence of magnetic field was attempted by Michiyoshi *et al.* [1] in 1975. After that, an experimental study of pool boiling of potassium under a magnetic field (maximum intensity: 0.7T) was carried out by Fujiie *et al.* [2]. They concluded that the nucleation in the wall cavity and the incipient boiling superheat are not influenced by the Lorentz force. Effects of magnetic field on the motion of a single nitrogen bubble rising through mercury were experimentally studied by Mori *et al.* [3]. They concluded that the effect of magnetic flux density B on the rise velocity depends largely on the radius of bubble. When the bubble diameter is 3 mm, the rise velocity decreases monotonously with the increase of B. However, for bubble of 1 mm dia, the rise velocity increases once, but it starts to decrease afterwards with the increase of B. Wagner *et al.* [4] and Lykoudis [5] dealt with an analytical study of the bubble growth under a spherically symmetric magnetic field using a spherical bubble growth model, and Wong *et al.* [6] also attempted an analytical study by considering the growth of an ellipsoidal bubble. All of them connected the behavior of bubble growth with the pool boiling heat-transfer coefficient by accounting for the bubble Reynolds number which appears to be the most important factor in model of Forster and Zuber [17].

The natural convection heat transfer under a magnetic field was studied by Dunn [7]. In his paper, the analytical model proposed by Lykoudis and Dunn [8] was examined by comparing with the experimental data of Michiyoshi *et al.* [1].

Many investigators have been studying about the pool boiling heat transfer, but a major unknown is the effect of magnetic field on the boiling characteristics of liquid metals, for lack of reliable experimental data.

This paper presents the reproducible experimental data of pool boiling heat transfer from a horizontal plane heater in pure mercury pool under various

system pressures and liquid levels in the presence of an applied magnetic field of which direction is parallel to the direction of gravity, and it is another purpose of this paper to get a key to understand the mechanism of boiling heat transfer and to apply the boiling phenomena to nuclear power system, by considering the action of magnetic field.

EXPERIMENTAL APPARATUS AND PROCEDURES

The schematic diagram of experimental apparatus is shown in Fig. 1, which consists of pool boiling vessel (test section), condensers, surge tank, vacuum systems and magnet. The surge tank is a large tank which may smooth down any large pressure fluctuations in the pool boiling vessel, and it is about forty times as large as a volume of the vessel. The diffusion pump is used to evacuate all contaminating gases from the system in addition to the rotary pump and then the system can be charged with pure argon. For the pressure gauge we use a mercury manometer and a pirani gauge. The dimension of magnetic pole-piece is $200 \times 1000\,mm^2$, and the maximum intensity of magnetic field of 0.9T can be obtained between the pole-piece gap of 150 mm wide.

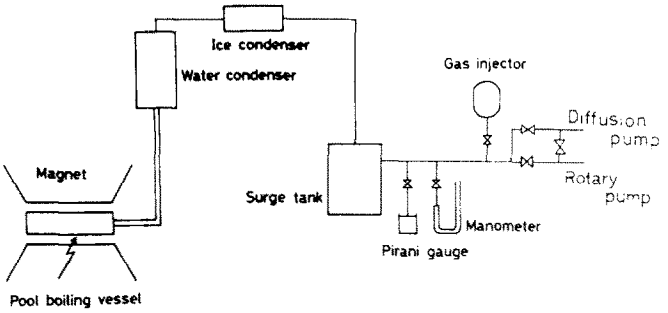

FIG. 1. Schematic diagram of experimental apparatus.

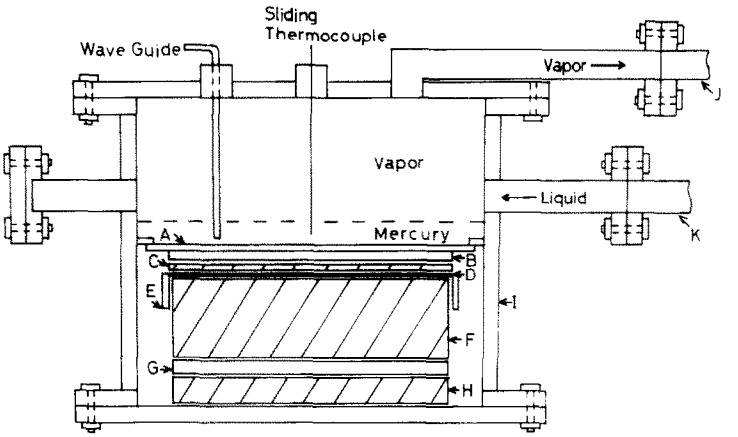

FIG. 2. Boiling apparatus. A. 316 stainless steel boiling surface. B. Copper heat conductor. C. Electric insulation (boron nitride). D. Nichrome heater. E. Copper electrode. F. Mica sheet. G. 316 stainless steel plate. H. Mica sheet. I. 304 stainless steel boiling tank. J. Connecting tube to vapor condenser. K. Connecting tube from vapor condenser.

Figure 2 shows the pool boiling vessel which consists of a heating section and a type 304 stainless steel tank of mercury having rectangular cross section of $50 \times 130\,mm^2$ and 50 mm high. Mercury vapor freed at the liquid vapor interface streams into a water condenser and returns to the boiling vessel after a change of phase. Heat input is conducted to mercury through the flat plate (type 316 stainless steel) A bonded with the copper plate B. There is an electrical insulated plate (boron nitride) C between the plate B and the heating element D which is made use of a nichrome plate and heated by supplying D.C. current. An outside heat loss from the heating element can be calculated by measuring the temperature difference of the two ends of stainless steel plate G provided between two thermal insulators F and H. A sliding thermocouple (stainless steel sheathed chromel–alumel thermocouple of 0.25 mm O.D.) is utilized to measure the vertical temperature distribution of liquid mercury. A waveguide method and a stethoscope are used for the purpose of boiling detector. However, boiling detection for a liquid level above the heating surface less than 5 mm is carried out with a visual method, because the waveguide rod becomes a nucleation site. As to a waveguide method, the propagation of acoustic and ultrasonic waves through a stainless steel rod of 5 mm O.D., which is immersed in mercury, is detected with a piezo microphone

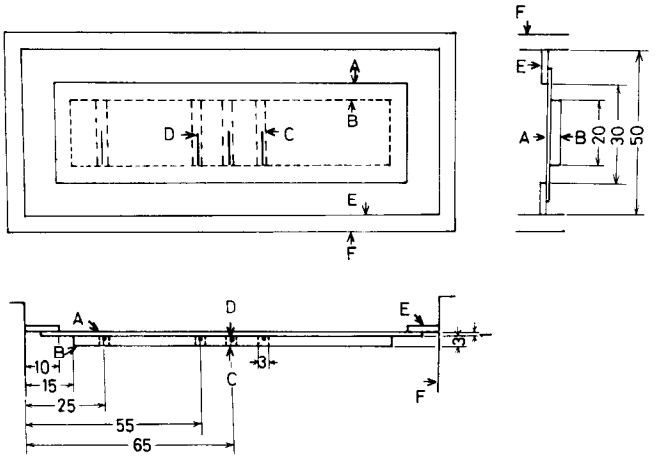

FIG. 3. Details of heating section (dimension in millimeter). A. 316 stainless steel boiling surface. B. Copper heat conductor. C. Copper element for thermocouple. D. Thermocouple. E. 304 stainless steel plate. F. 304 stainless steel boiling tank.

(barium titanate) connected with a tip of rod outside the boiling vessel. A mercury level above the heating surface is set with an electrical resistance type probe. Moreover, three glass windows are equipped at two sides ($20 \times 50\,mm^2$) and one upside ($50 \times 130\,mm^2$) of the vessel for the purpose of the observation of free surface of mercury.

Figure 3 shows a detail of the heating surface. The effective heating area is $20 \times 100\,mm^2$ within a polished surface $30 \times 110\,mm^2$ of a type 316 stainless steel A. The framed plate E is set for preventing the mercury from being separated into droplets. The stainless steel plate A and the copper B are bonded with the explosion-bonded clad method to keep the uniformity of heat flux across the heating surface. Unground type sheathed chromel–alumel thermocouples (0.25 mm O.D.) are used for measurements of internal heater temperature. These thermocouples are arranged at three points near the midpoint and 1 point near the end of the heater. The temperature of the heating surface (boiling surface) is determined by evaluating the position of thermocouples embedded in the copper plate B.

The heating surface is first polished with emery paper of fine grade every experiment and cleaned with acetone and distilled water, and then a certain quantity of distilled mercury is poured onto the heating surface. To begin a run, the auxiliary heater is turned on. As the mercury pool temperature approaches the saturation temperature corresponding to the system pressure, the power to the auxiliary heater is decreased to a very small heat input in comparison with a heat flux of the test heater.

The physical properties of mercury were taken from Schmücker's report [16].

RESULTS AND DISCUSSION

A preliminary test was performed with distilled water as the test fluid and the results were compared with those obtained by other investigators [9, 10], as shown in Fig. 4. The present boiling curve agrees well with Nishikawa's correlation [9]. Since the three thermocouples near the midpoint of the test heater showed similar tendency, one of the three thermocouples is used for arrangements of data.

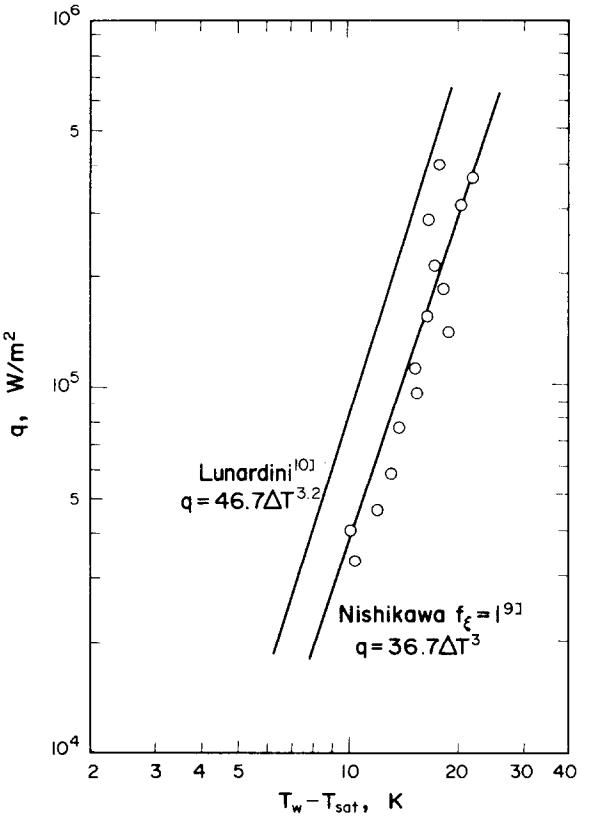

FIG. 4. Boiling curve of water for 40 mm liquid level and 760 torr system pressure.

Figures 5(a) and (b) show the vertical distributions of mercury temperature under boiling upwards from the heating surface, which were obtained by using the sliding thermocouple. The liquid level above the heating surface is 35 mm under the surface heat flux

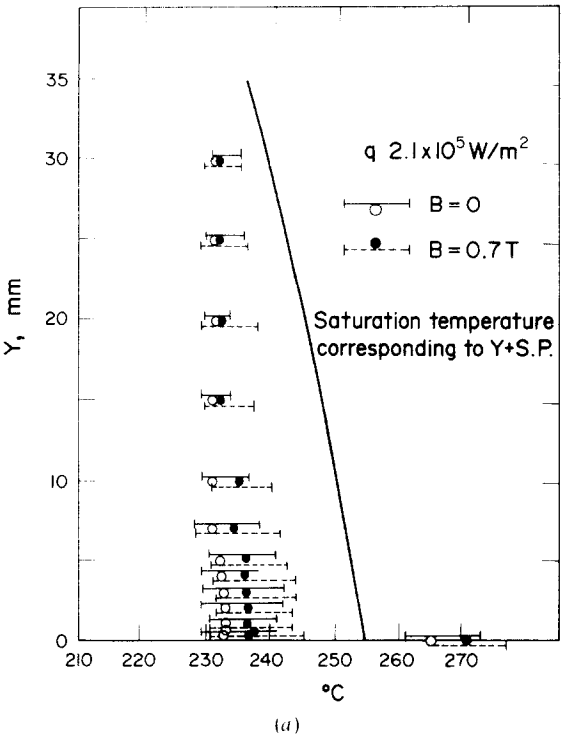

FIG. 5. (a) Vertical distribution of liquid temperature for 35 mm liquid level and 50 torr system pressure. (b) Vertical distribution of liquid temperature for 6 mm liquid level and 50 torr system pressure.

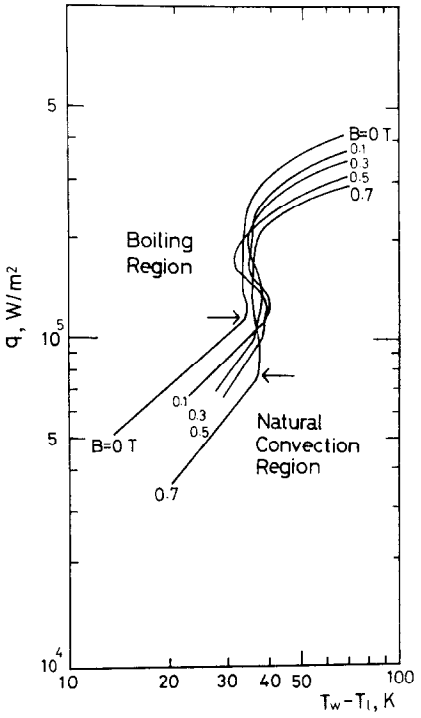

FIG. 6. Boiling curve of mercury under magnetic field for 35 mm liquid level and 50 torr system pressure. Incipient boiling is generated at a point marked with an arrow.

of 2.1×10^5 W m^{-2} in Fig. 5(a), and 6 mm under 8.0×10^4 W m^{-2} in Fig. 5(b). In both figures, the liquid and the heating surface temperature in the presence of magnetic field are higher than those in the case of $B = 0$. This is due to the suppression of flow by the Lorentz force. The liquid temperature is almost uniform everywhere except near the heating surface.

Boiling curves for 35 mm liquid level and 50 torr system pressure are shown in Fig. 6. The surface heat flux q is defined by dividing the heat input into the heater eliminated the outside heat loss by the heating surface area. The liquid temperature T_l represents the temperature measured at the fixed position of 20 mm above the heating surface where the liquid temperature is almost constant as shown in Fig. 5(a). This definition of T_l is the same as that in Figs. 7(a) and (b).

It can be seen that in both natural convection and boiling regions the presence of magnetic field, as a whole, reduces the heat-transfer coefficient as compared with the case of $B = 0$ at the fixed surface heat flux. The tendency of the effect of magnetic field on the heat transfer by natural convection is the same as Michiyoshi *et al.*'s result [1] for a horizontal cylinder.

The reduction of heat transfer in the boiling region seems due to the suppression of liquid being agitated by bubbles, if we may apply Mori *et al.*'s result [3] which showed that the rise velocity of bubble decreases monotonously with the increase of B. The effect of system pressure on the boiling curves is shown in Figs. 7(a) ($B = 0$) and 7(b) ($B = 0.7$T). The boiling curve may be divided into the following classes: (1) natural convection region, (2) low heat flux boiling region (intermittent boiling), and (3) high heat flux boiling region. In the natural convection region, the slope of curve q vs $T_w - T_l$ is

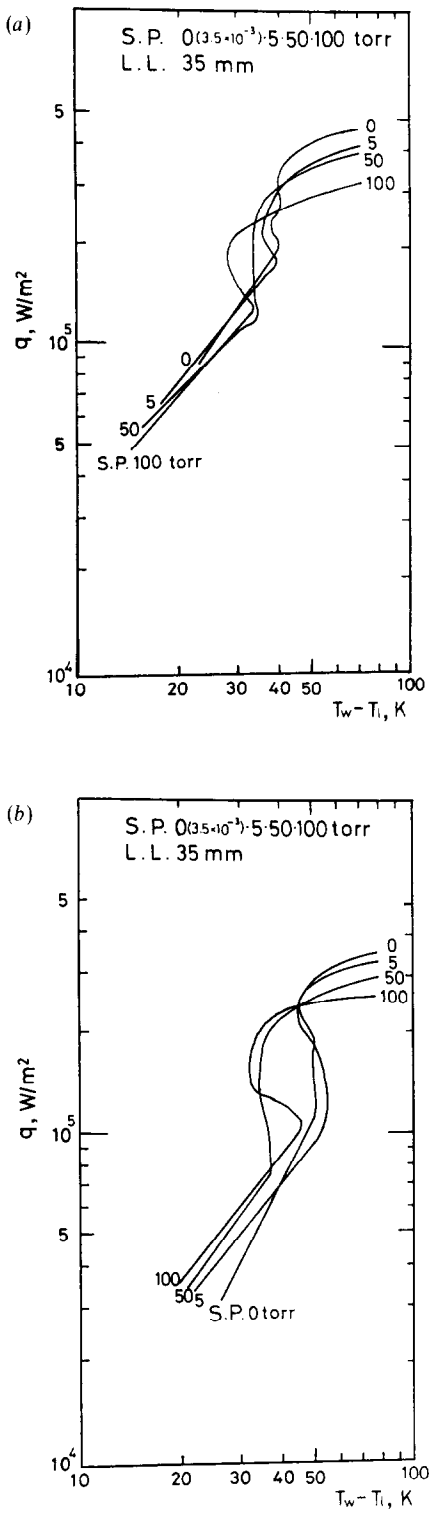

FIG. 7. (a) Effect of system pressure on boiling of mercury under non-magnetic field ($B = 0$). (b) Effect of system pressure on boiling of mercury under magnetic field ($B = 0.7$T).

about 5/4, and the system pressure affects much more the heat transfer under magnetic field than non-magnetic field, because the Lorentz force becomes stronger as the system pressure is lowered since the electrical conductivity of liquid metal increases with decreased liquid temperature (= saturation temperature corresponding to the system pressure). In the low heat flux boiling region, the slope of boiling curve q vs $T_w - T_l$ shows negative regardless of the presence of magnetic field, because the agitation of bubbles becomes more violent with increasing the heat flux. In the high heat flux boiling region, the boiling curve looks like that of film boiling for ordinary liquid such as water. As the system pressure is raised, the curve comes down under magnetic field as well as non-magnetic field. This represents the reduction of burnout heat flux. In this region the boiling curve, in general, differs from that of water and also sodium. This may be due to that the boiling curve is different by wetting and nonwetting degrees of the heating surface (see [11]).

Figure 8 shows the effect of magnetic flux density on the incipient boiling heat flux in the case of 35 mm liquid level. The incipient boiling heat flux decreases with increasing the magnetic flux density, because the heating surface temperature and the thermal boundary layer thickness adjacent to the heating surface increase by virtue of the Lorentz force at the fixed surface heat flux (see [1]). Two curves of $q_{IB}/q_{IB\,B=0}$ are drawn for 100 torr and very small system pressure to see easily this diagram. Figure 9 shows effects of liquid level above the heating surface and magnetic flux density on the incipient boiling heat flux at 100 torr system pressure. The effect of magnetic flux density becomes much smaller when the liquid level is less than 7 mm. From these experimental results it should be noted that the magnitude of the Lorentz force is different for different thickness of liquid layer which changes the flow circulation pattern. Figure 10 shows effects of magnetic flux density on the magnitude of the wall superheat $T_w - T_{w\,sat}$ of heating surface when the incipient boiling is generated. Although attention was paid to detect the incipience of boiling, the experimental data scatter in some degree. This may be due to the fact that an incipient boiling is not always generated at the point imbedded the thermocouple. Nevertheless, it can be seen from this figure that the incipient boiling wall superheat under the magnetic field ($B = 0.9$T) is, as a whole, a little larger than the case of $B = 0$.

Relationship between the boiling heat-transfer coefficient α and the liquid level is shown in Fig. 11, where α is the heat flux q divided by $T_w - T_{sat}$. When the liquid level was kept at 3 mm and 5 mm, a large bubble of about 25 mm dia was observed on the heating surface under magnetic and non-magnetic fields [see Fig. 15(a)]. The heat-transfer coefficient takes the maximum value at the surface heat flux which starts to generate large bubbles for the 3 mm liquid level, but a number of large bubbles reduce the heat-transfer coefficient as the heat flux is increased. Results of Nishikawa *et al.* [12], Kusuda *et al.* [13], Patten [14] and Tolubinsky [15] with ordinary liquids (water etc.) indicate that the boiling

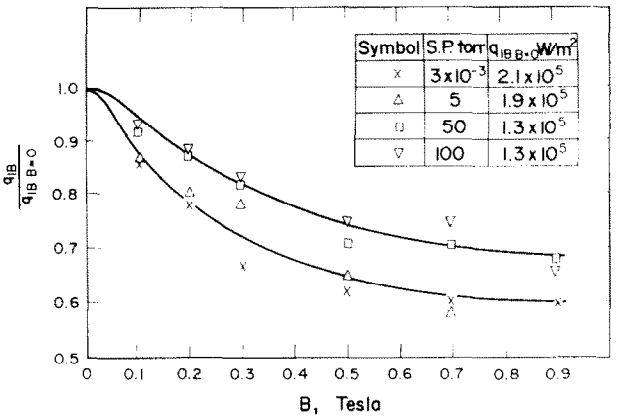

FIG. 8. Effect of magnetic flux density on incipient boiling heat flux for 35 mm liquid level.

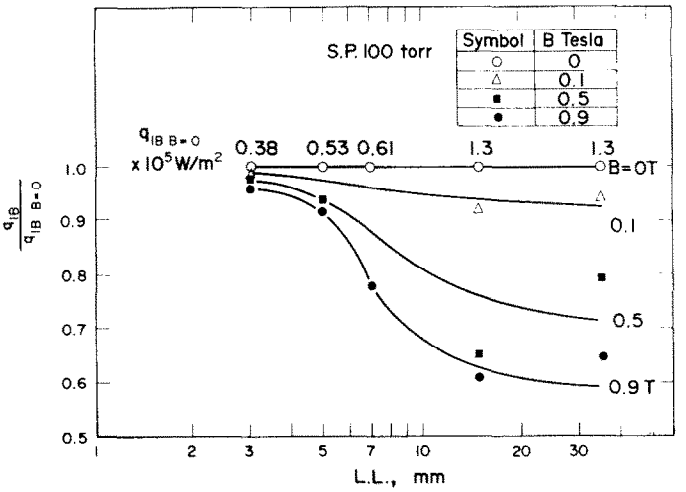

FIG. 9. Effect of magnetic flux density and liquid level on incipient boiling heat flux.

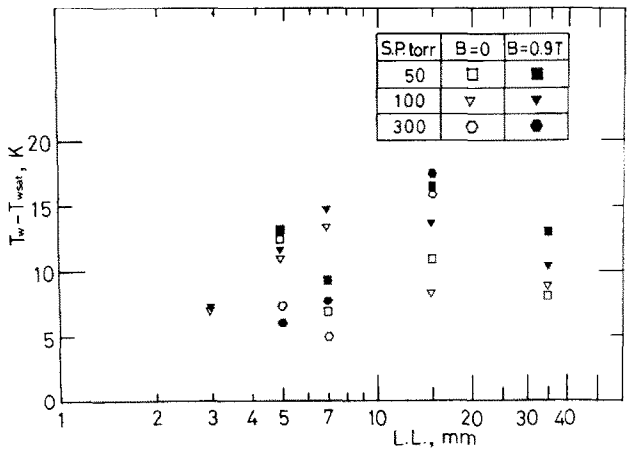

FIG. 10. Incipient boiling wall superheat of mercury.

heat-transfer coefficient for thin liquid layers less than 5 mm is larger than that of pool boiling for much thicker liquid layers at the fixed heat flux, but this is not the case for thin layers of pure mercury as shown in Fig. 11. This may be due to the effect of the degree of wetting of the heating surface.

The boiling test was also carried out over a long period to investigate effects of surface aging, which is especially important for thin liquid layer in the case of which the system gas (cover gas) often directly contacts the heating surface. After a long running test, the heat-transfer coefficient decreased much

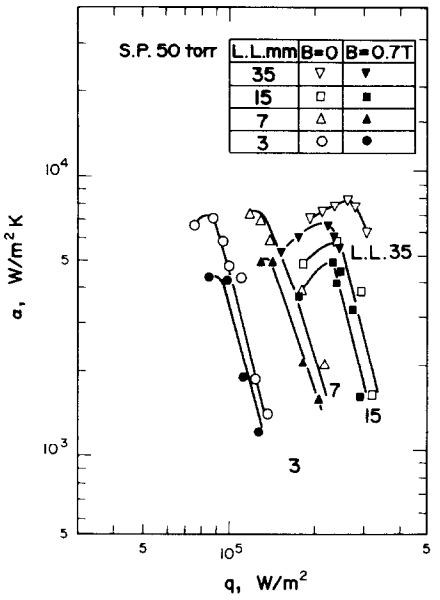

FIG. 11. Heat transfer for pool boiling of mercury.

compared with that obtained by a short running test, for example the incipient boiling heat flux for 3 mm liquid level caused burnout after a long running test and the heating surface became semi-dark.

The effect of magnetic flux density on the burnout heat flux for 35 mm liquid level is shown in Fig. 12. The burnout heat flux was determined when the heating surface temperature rose rapidly and monotonously (rising rate is about 5 K/s) at constant heat flux, and if the power input was not cut off, the heater went to burnout. The burnout heat flux q_{crit} decreases with increasing the magnetic flux density, and $q_{crit}/q_{crit\,B=0}$ becomes about 75% when $B = 0.9$T. This result is caused by the suppression of liquid flow toward the heating surface by virtue of the Lorentz force after the bubble departed from the heating surface. From scattered experimental data, the effect of system pressure on $q_{crit}/q_{crit\,B=0}$ is not clear. Figure 13 shows effects of magnetic flux density and liquid level on the burnout heat flux. The burnout heat flux decreases with decreasing the liquid level, and the effect of magnetic field on the

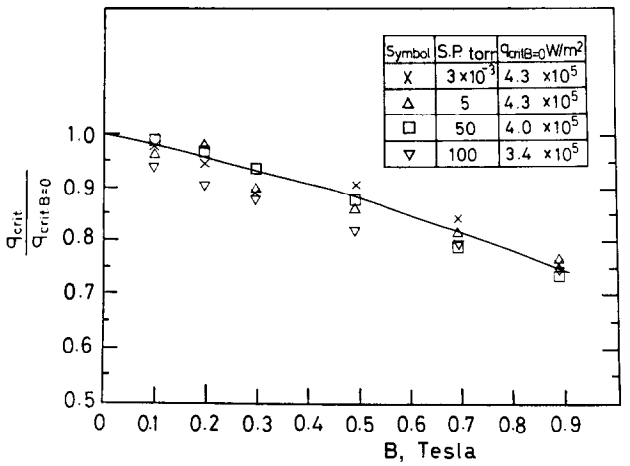

FIG. 12. Effect of magnetic flux density on burnout heat flux for 35 mm liquid level.

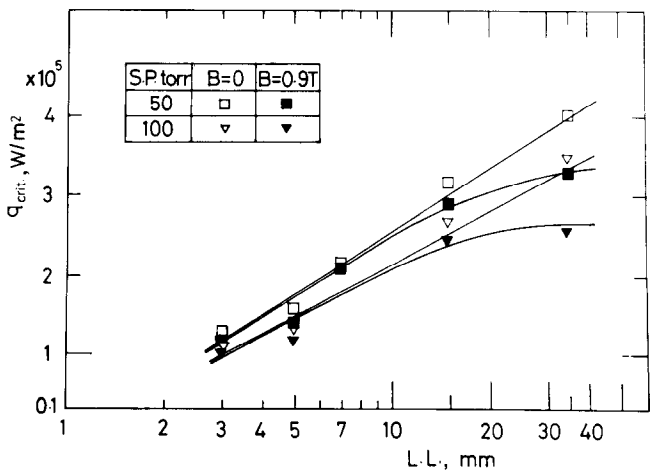

FIG. 13. Effect of liquid level on burnout heat flux.

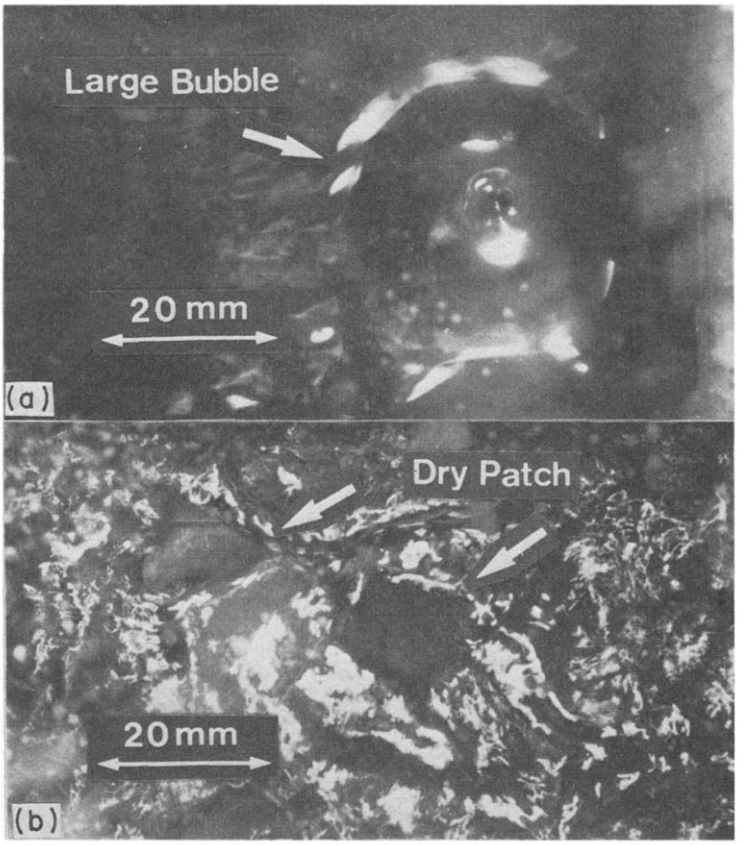

FIG. 14. Photograph of large bubble (top view). $q = 1.0 \times 10^5$ W m^{-2}, system pressure = 50 torr, liquid level = 3 mm and $B = 0$.

burnout heat flux becomes much smaller as the liquid level is lowered.

Figures 14 and 15 show photographs of typical large bubble mentioned above, which are 20–30 mm in diameter and generated only when the liquid level above the heating surface is less than 5 mm. Results of visual study are as follows: (1) Shape of bubble under magnetic field ($B \leqslant 0.9$T) is similar to that of $B = 0$. (2) Dry part of heating surface appears after the disappearance of large bubble [see Fig. 14(b)]. (3) Surface wave due to the bubble generation is suppressed under magnetic field. (4) When a thermocouple and a waveguide rod are immersed in mercury layer, they become a nucleation site. (5) As for a behavior of bubble disappearance, some bubbles shrink and some split open to liquid particles in all directions for $B = 0$ [see Fig. 15(b)], but almost all shrink for $B \neq 0$. (6) Bubble growth rate measured by using a high speed camera under magnetic field is a little small compared with that of $B = 0$, as shown in Fig. 16. This fact seems due to the motion of liquid adjacent to the root of large bubble being suppressed by the Lorentz force as compared with the case of $B = 0$.

CONCLUSION

Pool boiling heat transfer was experimentally studied on a horizontal plane heater immersed in mercury pool under various system pressures and liquid levels in the presence of magnetic field. With increasing the magnetic flux density, both the incipient boiling heat flux and the burnout heat flux decrease in comparison with those for the non-magnetic field. When the liquid thickness above the heating surface is thin, however, the magnetic field affects little the incipient boiling heat flux and the burnout heat flux. When the liquid thickness is less than 5 mm, the formation of large bubbles of about 25 mm dia is observed. The bubble growth rate of large bubble is a little small under magnetic field compared with that of $B = 0$.

Acknowledgement—This research was partly supported by the Fundamental Studies on Two-Phase Flow Characteristics for Thermal Design of Fusion Reactor Blanket supported by the Ministry of Education of Japanese Government.

REFERENCES

1. I. Michiyoshi, O. Takahashi and A. Serizawa, Natural convection heat transfer from a horizontal cylinder to mercury under magnetic field, *Int. J. Heat Mass Transfer* **19**, 1021–1029 (1976).
2. Y. Fujiie, Y. Fukuzawa and H. Takatsu, Influence of magnetic field on boiling of stagnant potassium, *J. Nucl. Sci. Technol.* **13**, 483–491 (1976).
3. Y. Mori, K. Hijikata and I. Kuriyama, Experimental

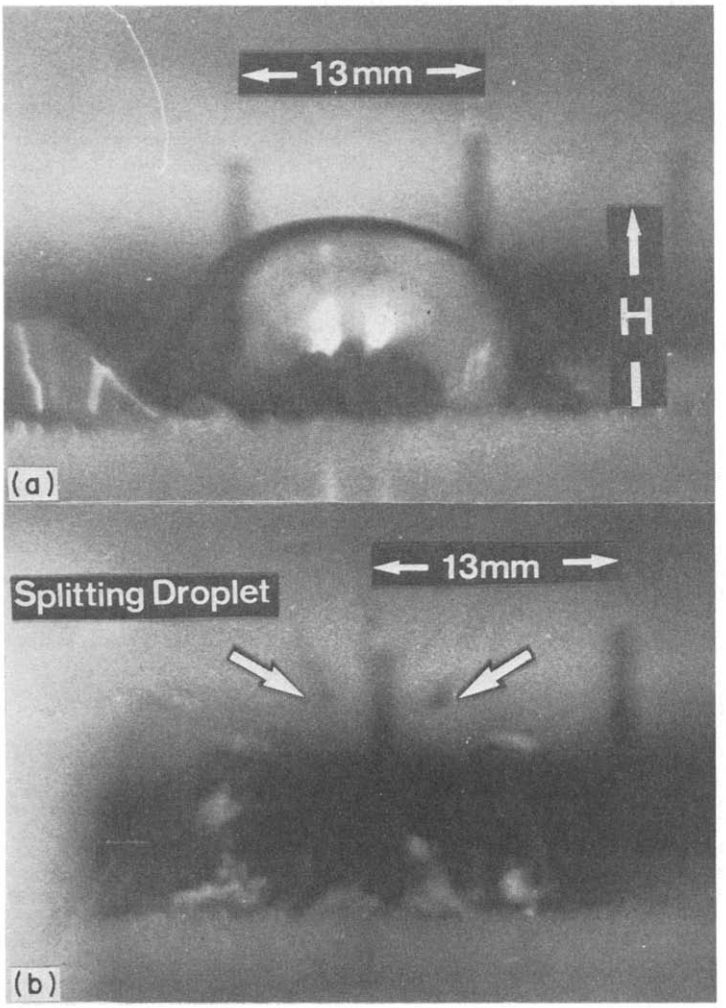

FIG. 15. Photograph of large bubble (side view). $q = 1.0 \times 10^5\ \mathrm{W\,m^{-2}}$, system pressure = 50 torr, liquid level = 3 mm and $B = 0$.

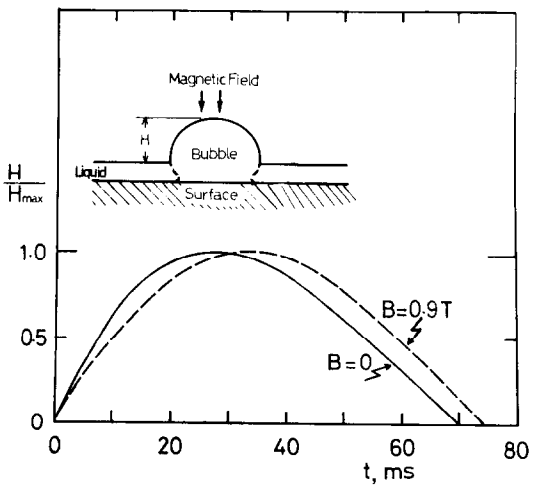

FIG. 16. Effect of magnetic field on growth rate of large bubble. $q = 1.0 \times 10^5\ \mathrm{W\,m^{-2}}$, system pressure = 50 torr and liquid level = 3 mm.

study of bubble motion in mercury with and without a magnetic field, *J. Heat Transfer* **99C**, 404–410 (1977).
4. L. Y. Wagner and P. S. Lykoudis, The effect of liquid inertia on bubble growth in the presence of a magnetic field, Paper No. AIChE-37, in *Proceedings of the ASME AIChE 16th National Heat Transfer Conf.* (1976).
5. P. S. Lykoudis, Bubble growth in the presence of a magnetic field, *Int. J. Heat Mass Transfer* **19**, 1357–1362 (1976).
6. C. P. C. Wong, G. C. Vliet and P. S. Schmidt, Magnetic field effect on bubble growth in boiling liquid metals, *J. Heat Transfer* **100**, 466–472 (1978).
7. P. F. Dunn, A model of MHD natural-convection heat transfer from a finite cylinder, ASME Paper No. 78-WA/HT-24 (1978).
8. P. S. Lykoudis and P. F. Dunn, Magneto-fluid-mechanic heat transfer from hot film probes, *Int. J. Heat Mass Transfer* **16**, 1439–1452 (1973).
9. K. Nishikawa, Y. Fujita and T. Matsuo, On the correlation of nucleate boiling heat transfer based on the bubble population, *Trans. Japan. Soc. Mech. Engrs* **41**, 2141–2150 (1975).
10. V. J. Lunardini, Jr., An experimental study of the effect of a horizontal magnetic field on the nucleate pool

boiling of water and mercury with 0.02% Mg and 0.0001% Ti, Ohio State University, Ph.D. Dissertation (1963).
11. O. E. Dwyer, *Boiling Liquid–Metal Heat Transfer*, pp. 287 and 332. American Nuclear Society, Hinsdale, Illinois (1976).
12. K. Nishikawa, H. Kusuda, K. Yamasaki and K. Tanaka, Nucleate boiling at low liquid levels, *Trans. Japan. Soc. Mech. Engrs* **32**, 1255–1264 (1966).
13. H. Kusuda and K. Nishikawa, A study on nucleate boiling in liquid film, *Trans. Japan. Soc. Mech. Engrs* **34**, 944–949 (1968).
14. T. D. Patten and W. A. Turmeau, Some characteristics of nucleate boiling in thin liquid layers, in *Heat Transfer* 1970, Paris, Vol. V, B2.10, Elsevier (1970).
15. V. I. Tolubinsky, V. A. Antoneko and Ju. N. Ostrovsky, Heat transfer at liquid boiling in thin films, International Centre for Heat and Mass Transfer 1978 International Seminar, Yugoslavia (1978).
16. H. Schmücker, Sieden von Quecksilber im senkrechten Rohr bei Zwangskonvektion und niedrigen Drücken, Technische Universität München. Dr.-Ing. Dissertation (1974).
17. H. K. Forster and N. Zuber, Dynamics of vapor bubble and boiling heat transfer, *A.I.Ch.E. Jl* **1**, 531–535 (1955).

TRANSFERT THERMIQUE AVEC EBULLITION EN RESERVOIR POUR UN CHAUFFOIR PLAN ET HORIZONTAL ET DU MERCURE SOUS UN CHAMP MAGNETIQUE

Résumé—On présente des résultats expérimentaux reproductibles pour l'ébullition du mercure en réservoir, en présence d'un champ magnétique de direction parallèle à celle de la pesanteur, sous différentes pressions et avec un chauffoir plan et horizontal. Lorsque la densité du flux magnétique augmente, l'apparition de l'ébullition et le flux critique diminuent en comparaison du cas où le champ magnétique est nul. Néanmoins cette différence est très réduite lorsque l'épaisseur du liquide au dessus de la surface est mince. On discute aussi les résultats d'une étude visuelle de l'ébullition du mercure.

WÄRMEÜBERGANG AN QUECKSILBER BEIM BEHÄLTERSIEDEN AN EINER HORIZONTALEN PLATTE UNTER EINWIRKUNG EINES MAGNETISCHEN FELDES

Zusammenfassung—Für den Wärmeübergang an Quecksilber beim Behältersieden an einer horizontalen Platte werden reproduzierbare Meßergebnisse mitgeteilt. In Gegenwart eines dem Schwerefeld parallelen magnetischen Feldes wurden Systemdruck und Flüssigkeitsstand variiert. Mit zunehmender magnetischer Flußdichte nehmen sowohl die Wärmestromdichte ab, bei der das Sieden einsetzt, wie auch die kritische Wärmestromdichte (im Vergleich mit den Werten ohne magnetisches Feld). Bei geringer Flüssigkeitshöhe über der Heizfläche ist der Einfluß des magnetischen Feldes auf die beiden vorerwähnten Wärmestromdichten gering.

Weiter werden die Ergebnisse einer visuellen Studie des Quecksilber-Siedens diskutiert.

ТЕПЛОПЕРЕНОС ОТ ГОРИЗОНТАЛЬНОГО ПЛОСКОГО НАГРЕВАТЕЛЯ К РТУТИ В МАГНИТНОМ ПОЛЕ ПРИ КИПЕНИИ В БОЛЬШОМ ОБЪЁМЕ

Аннотация — Представлены воспроизводимые экспериментальные данные по теплопереносу при кипении в большом объёме от горизонтального плоского нагревателя к ртути при различных давлениях и уровнях жидкости в системе, находящейся в магнитном поле, направление которого совпадает с направлением силы тяжести. При увеличении плотности магнитного потока как величина теплового потока, при которой возникает кипение, так и величина критического теплового потока уменьшаются по сравнению со случаем отсутствия магнитного поля. Однако, в случае небольшой толщины слоя жидкости на поверхности нагрева магнитное поле оказывает слабое влияние на указанные величины. Проведено также обсуждение результатов визуального изучения процесса кипения ртути.